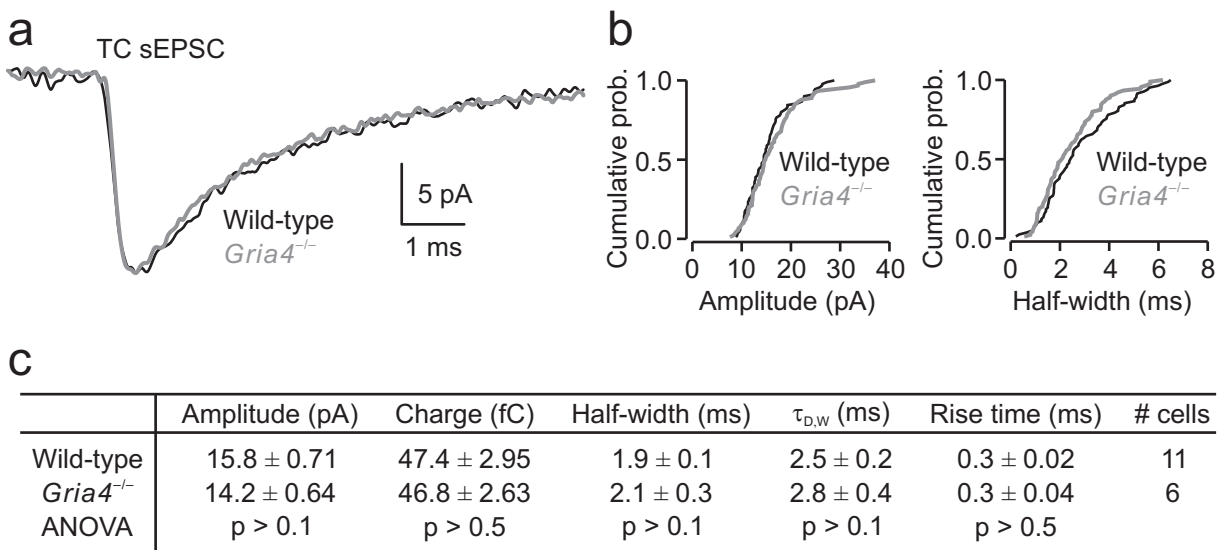


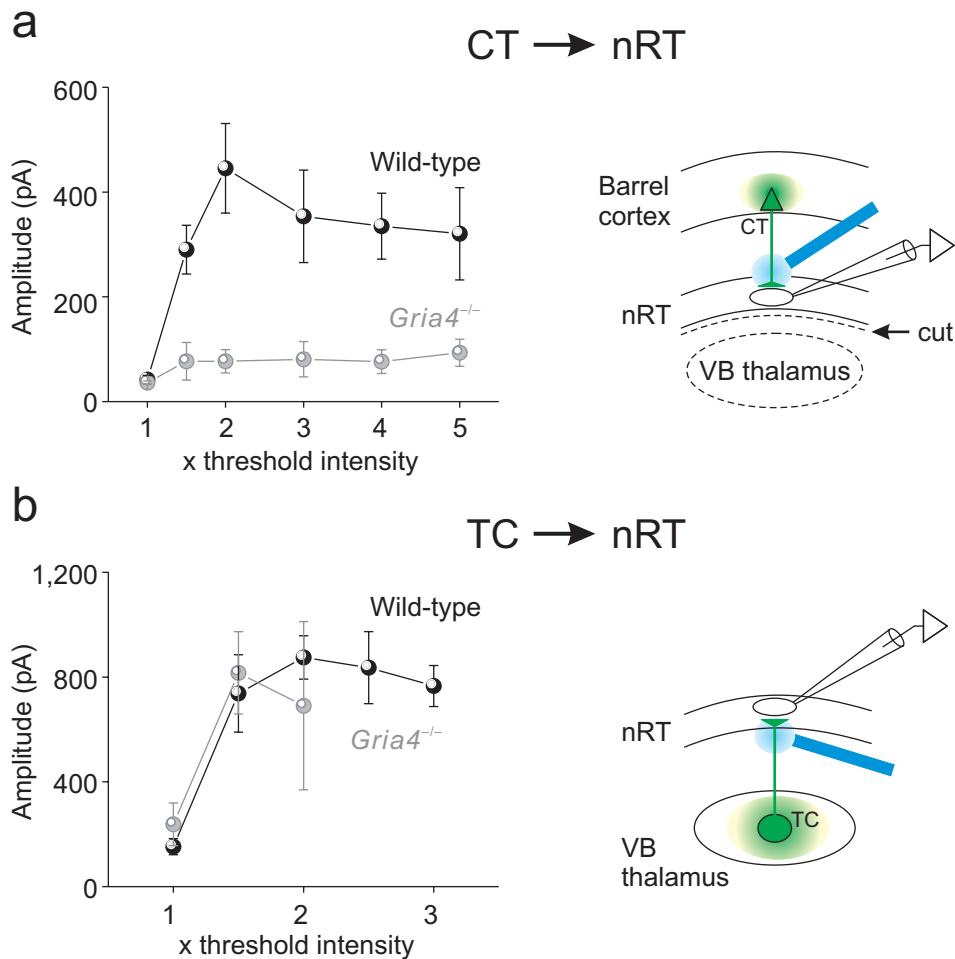
SUPPLEMENTARY MATERIAL

A new mode of corticothalamic transmission revealed
in the GluA4 knockout model of absence epilepsy

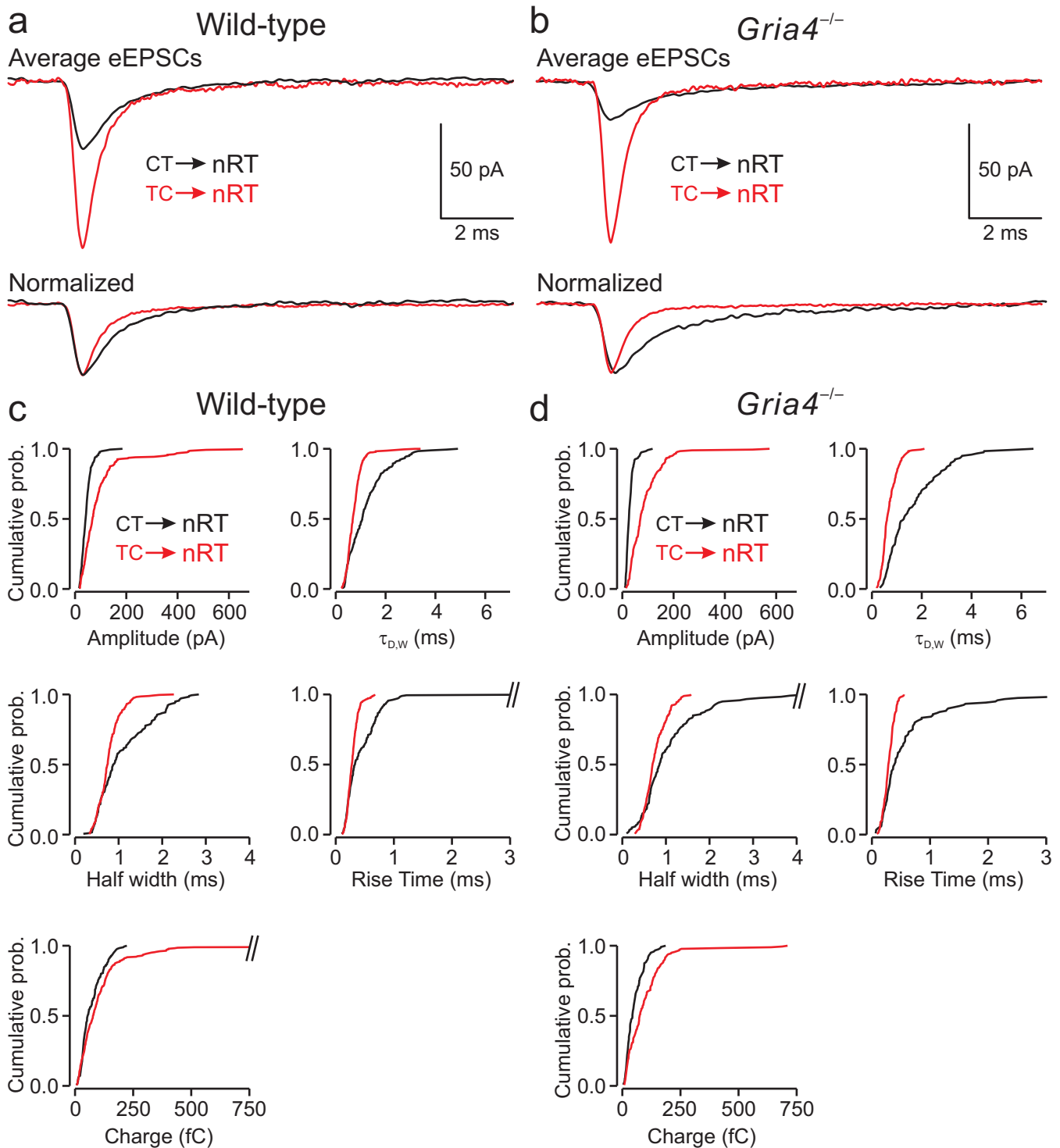
Jeanne T. Paz, Astra S. Bryant, Kathy Peng, Lief Fenno, Ofer Yizhar, Wayne N. Frankel, Karl Deisseroth and John R. Huguenard



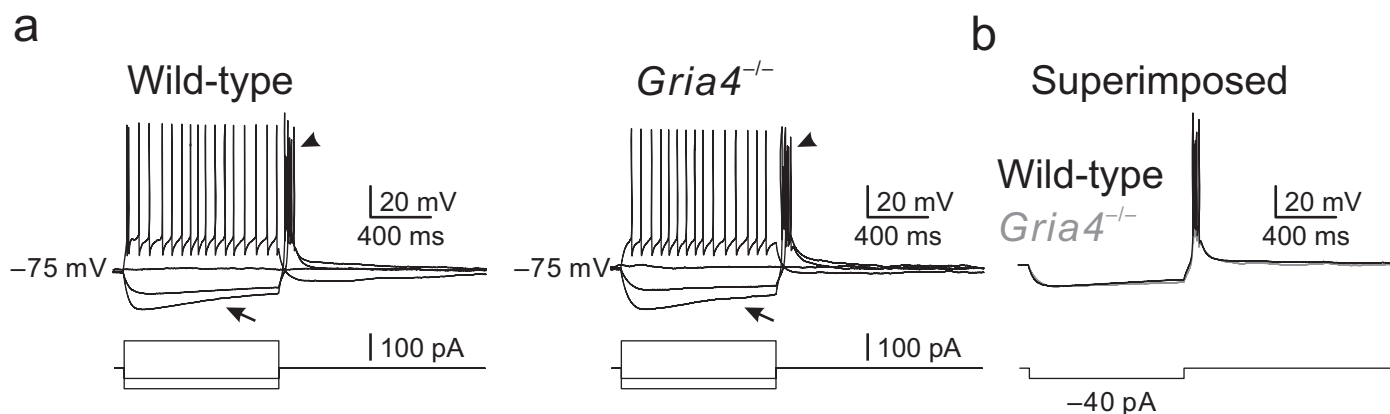
Supplementary Figure 1. Absence of AMPA receptor GluA4 does not alter synaptic excitation in TC neurons from VB thalamus. (a) Ensemble averaged sEPSCs from single TC cells from wild-type (black) and *Gria4^{-/-}* (gray) mice, plotted on the same time scale. (b) Cumulative probability histograms of isolated sEPSC amplitudes and half-widths (wild-type, n = 90 events; *Gria4^{-/-}*, n = 90 events) from the cells depicted in a show no changes in amplitude or kinetics between genotypes (p > 0.3, Kolmogoroff-Smirnoff test). (c) Quantification of the averaged amplitude, charge, half-width, double exponential weighted decay-time constant ($\tau_{D,W}$) and 10–90% rise-time of sEPSCs from 11 wild-type and 6 *Gria4^{-/-}* TC neurons. Error bars, s.e.m.



Supplementary Figure 2. In *Gria4*^{-/-} mice input–output relationships for evoked EPSCs are reduced in CT–nRT but not TC–nRT pathway. (a) Selective optical stimulation of CT axons evokes significantly ($p < 0.05$) smaller EPSCs in nRT neurons from *Gria4*^{-/-} ($n = 3$ cells) versus wild-type ($n = 5$ cells) mice. **(b)** Selective optical stimulation of TC axons evokes similar amplitude ($p > 0.3$) EPSCs in nRT neurons from *Gria4*^{-/-} ($n = 4$ cells) and wild-type ($n = 4$ cells) mice. Right panels in **a–b** depict schematic diagrams of the experimental configuration showing location of virus injection (green spots), recording electrode (in nRT) and laser stimulation (blue beam). In **a–b** we used the same experimental configurations as the ones illustrated on **Figs. 5** and **4**, respectively which were used to show that minimal EPSCs evoked by CT–nRT pathway are reduced in *Gria4*^{-/-} versus wild-type (**Fig. 5**) but those evoked by TC–nRT pathway are similar in both genotypes (**Fig. 4**). Statistical significance in **a–b**: one-way ANOVA test. Error bars, s.e.m.



Supplementary Figure 3. Comparison of EPSC properties in nRT evoked by optical stimulation of CT or TC axons. (a,b) Top traces: Averaged minimal EPSCs from single nRT cells evoked by optical stimulation of CT (black) or TC (red) axons from wild-type (a) and *Gria4*^{-/-} mice (b). Note the smaller amplitude of cortically evoked EPSCs compared with those evoked by TC stimulation. Bottom traces: normalized eEPSCs illustrating slower decay kinetics in cortically evoked EPSCs compared with those evoked by TC stimulation. (c,d) Cumulative probability histograms of isolated EPSCs in nRT from wild-type (c) and *Gria4*^{-/-} mice (d) evoked by optical activation of CT (black) or TC (red) axons. Cortically evoked EPSCs, versus those evoked by TC stimulation, showed differences in amplitude and kinetics in both wild-type and *Gria4*^{-/-} mice (c-d, $p < 10^{-10}$, Kolmogoroff-Smirnoff test).

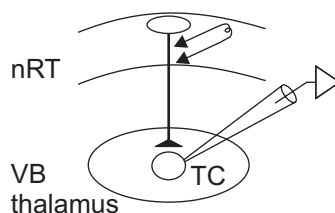


c

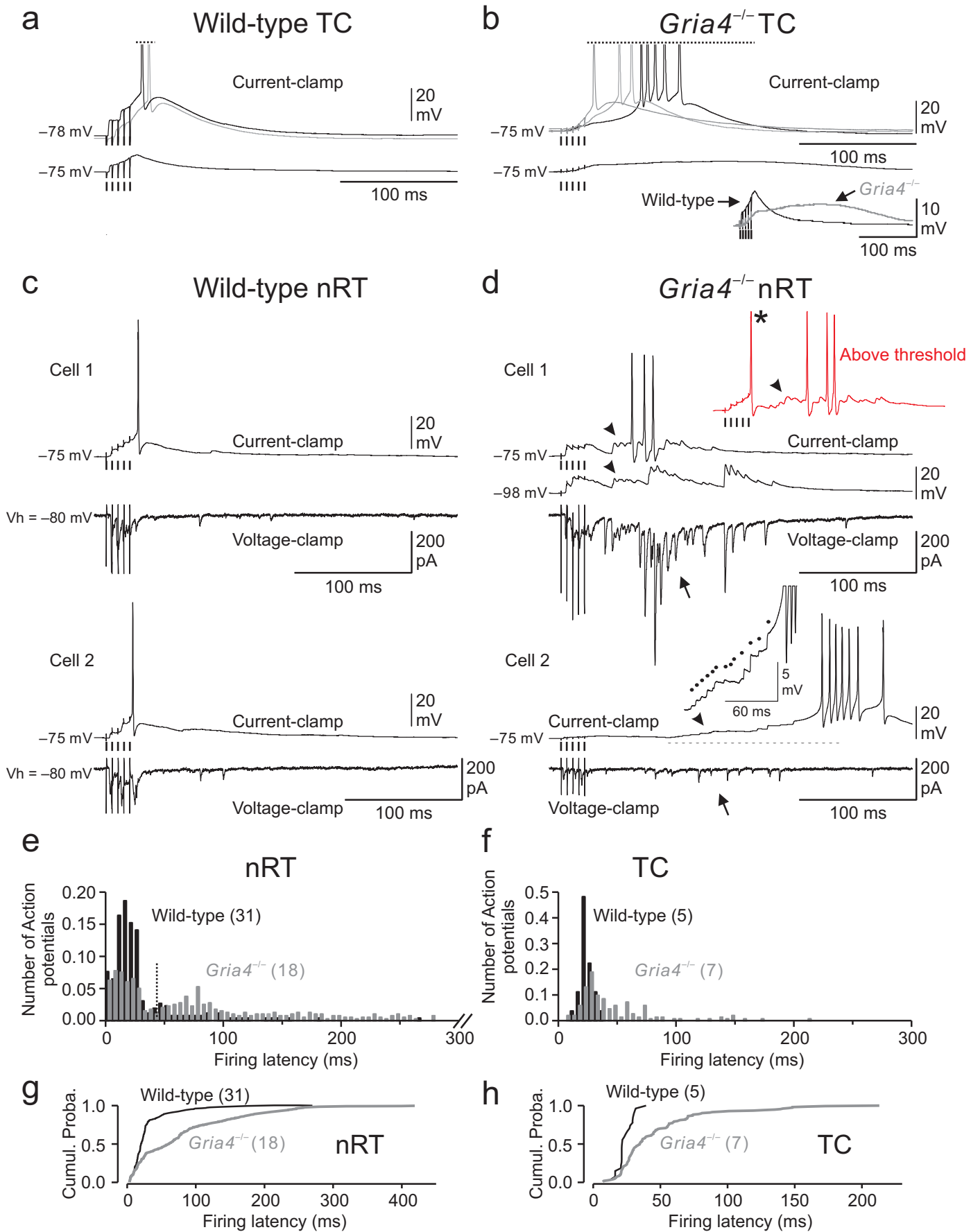
	V_m (mV)	R_{in} (M Ω)	τ_m (ms)	Action potential threshold (mV)	Action potential duration (ms)	# cells
Wild-type	-70.9 ± 1.0	212.7 ± 18.5	43.9 ± 2.9	-55.1 ± 0.7	2.5 ± 0.1	18
<i>Gria4</i> ^{-/-}	-70.3 ± 1.2	239.1 ± 24.0	41.7 ± 3.1	-54.4 ± 0.9	2.6 ± 0.1	12
ANOVA	$p > 0.5$	$p > 0.1$	$p > 0.5$	$p > 0.5$	$p > 0.1$	

d

	Amplitude (pA)	Charge (fC)	Half-width (ms)	Rise time (ms)	Decay time (ms)	Intensity (V)	# cells
Wild-type	-327.8 ± 63.7	$11,387 \pm 2,786$	17.7 ± 2.6	2.2 ± 0.2	46.0 ± 5.9	21.6 ± 3.1	14
<i>Gria4</i> ^{-/-}	-313.3 ± 64.6	$9,077 \pm 2,006$	17.5 ± 2.2	2.3 ± 0.2	49.0 ± 5.3	18.1 ± 1.3	24
ANOVA	$p > 0.5$	$p = 0.5$	$p > 0.5$	$p > 0.5$	$p > 0.5$	$p > 0.1$	

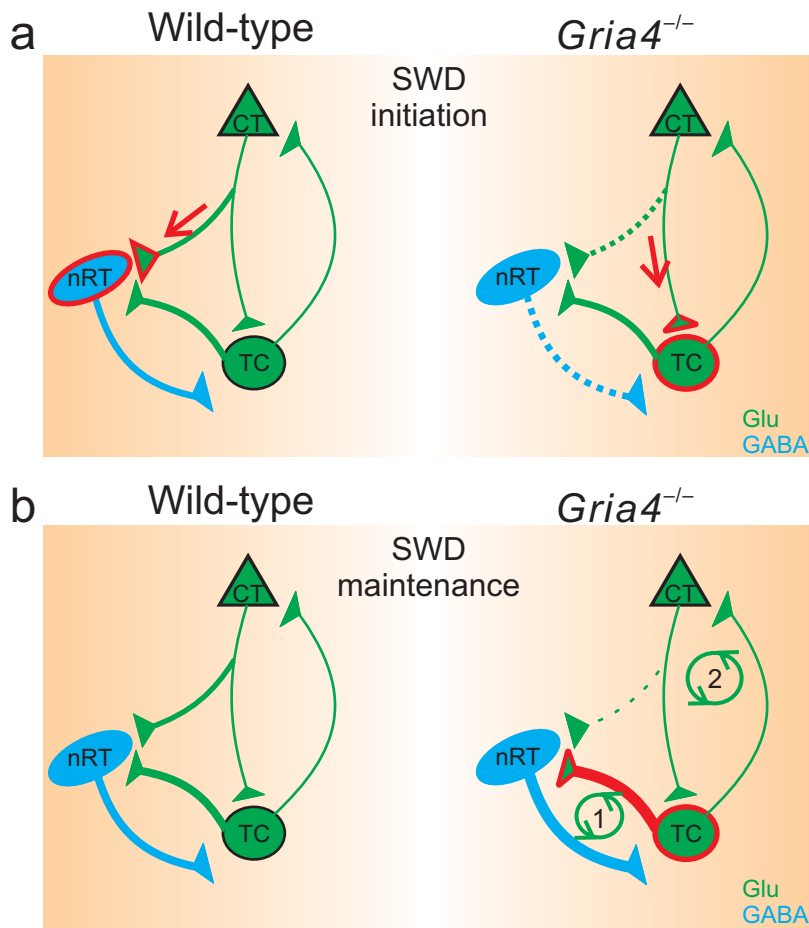


Supplementary Figure 4. VB TC neurons from wild-type and *Gria4*^{-/-} mice exhibit similar electrical membrane properties (a-c) and similar IPSCs evoked by nRT stimulation (d). (a) Voltage responses of representative wild-type) and *Gria4*^{-/-} VB TC relay neurons (top traces) to intracellular injection of positive and negative square current pulses (bottom traces). Wild-type and *Gria4*^{-/-} TC neurons exhibit similar hyperpolarization-activated depolarizing sag (arrows) and a similar post-inhibitory rebound burst of action potentials (arrowheads). (b) Top, superimposition of voltage responses to intracellular injections of -40 pA pulses (bottom trace) in TC neurons from wild-type and *Gria4*^{-/-} mice. Note similar membrane input resistance (R_{in}) and time constant (τ_m) in both genotypes. (c) The membrane resting potential (V_m), R_{in} , τ_m and action potential properties of TC neurons were similar in wild-type ($n = 18$ cells) and *Gria4*^{-/-} ($n = 12$ cells) mice. (d) IPSCs evoked in TC neurons by threshold stimulation of nRT fibers exhibited similar amplitude, charge and kinetics in wild-type and *Gria4*^{-/-} mice. The intensity of stimulation (Intensity) required to elicit IPSCs at threshold (i.e. presumably activating one presynaptic fiber) was similar in wild-type and *Gria4*^{-/-} mice. Inset, schematic diagram of the experimental configuration showing locations of the bipolar stimulating electrode (in nRT) and the recording electrode (in VB thalamus). Statistical significance: one-way ANOVA. All values are expressed as means \pm s.e.m.



Supplementary Figure 5

Supplementary Figure 5. Excitatory synaptic response in TC and nRT neurons evoked by electrical stimulations is enhanced in *Gria4*^{-/-} mice. (a–b) Evoked firing in TC neurons from wild-type (a, top traces) and *Gria4*^{-/-} (b, top traces) induced by stimuli at 200 Hz at firing threshold in the internal capsule. Grey and black traces are from different representative neurons. Action potentials were truncated (horizontal dashed lines in a and b). Subthreshold depolarizations (bottom traces in a and b, superimposed in the inset in b) evoked by synaptic stimulation lasted longer in *Gria4*^{-/-} mice. (c–d) Evoked responses from representative nRT cells from wild-type and *Gria4*^{-/-} mice evoked by threshold electrical stimulations (200 Hz, 5 shocks) of the internal capsule activating both CT and TC fibers projecting to nRT (see Methods). In the wild-type (c), synaptic stimulation typically induced one early (~25 ms) action potential firing. In *Gria4*^{-/-} (d), synaptic stimulation induced subthreshold short latency EPSPs, but led to late (> 40 ms) action potential firing. Early firing (asterisk) could be obtained by increasing stimulation intensity (red trace in d), likely resulting from antidromic activation of TC cells. The evoked late action potential firing was preceded by bursts of EPSPs (arrowheads in d) resulting from large amplitude and long-lasting (> 200 ms) EPSCs occurring at high-frequency (50–200 Hz) (arrows in d). Cell 2 in d: The current-clamp recording period indicated with a dashed line was expanded to show that the evoked late firing was preceded by temporal summation of small-amplitude depolarizing potentials (black dots). (e) In wild-type cells the synaptic stimulation failed to induce late bursts of EPSPs and EPSCs. (f) Pooled histograms normalized for the number of events showing the distribution of latencies of the evoked action potentials in nRT neurons with respect to the first stimulation artifact (wild-type, n = 263 action potentials from 31 neurons; *Gria4*^{-/-}, n = 400 action potentials from 18 neurons; bin size, 5 ms for both histograms). Note the unimodal distribution of latencies in wild-type (around ~17 ms) versus a bimodal distribution in *Gria4*^{-/-} (around ~17 ms and ~77 ms). In wild-type, only 15.6 % of events occurred > 45 ms; whereas in *Gria4*^{-/-}, 56% of events occurred > 45 ms. (g) Pooled histograms normalized for the number of events showing the distribution of latencies of the evoked action potentials in TC neurons with respect to the first stimulation artifact (wild-type, n = 27 action potentials from 5 neurons; *Gria4*^{-/-}, n = 154 action potentials from 7 neurons; bin size, 5 ms for both histograms). (g,h) Cumulative probability histograms of the evoked action potential latencies in nRT (g) and TC neurons (h) corresponding to values presented in e and f from nRT and TC, respectively, demonstrate prolonged firing in both nRT and TC neurons from *Gria4*^{-/-} mice (nRT, wild-type versus *Gria4*^{-/-}, p < 10⁻¹⁰; TC, wild-type versus *Gria4*^{-/-}, p < 10⁻⁴, Kolmogoroff-Smirnoff test). nRT and TC neurons were recorded from the same thalamic slices. The evoked action potential latency was calculated with respect to the first stimulation artifact for all the cells. Traces in a and c are temporally aligned. Traces in b and d are temporally aligned. In a–d the values of the membrane potential are indicated on the left. Holding membrane potential (V_h) was the same (-80 mV) for all the voltage-clamp recordings. Picrotoxin (50 μM) was included to block GABA_A receptors. GABA_B and NMDA receptor-mediated activity were intact. Differences in the evoked firing between wild-type and *Gria4*^{-/-} nRT and TC cells were confirmed at 1.5x, and 2x stimulation intensities (not shown). Number of cells is indicated in parentheses.



Supplementary Figure 6. New mode of corticothalamic transmission and seizure initiation revealed in *Gria4*^{-/-} mice. (a) Information transfer from cortex to thalamus: an unfair contest. In normal conditions (wild-type), synaptic strength in CT-nRT pathway is stronger than in CT-TC pathway. Thus CT inputs robustly excite GABAergic nRT neurons (red arrow) which, subsequently, inhibit relay TC neurons (b, left). In absence of GluA4 (*Gria4*^{-/-}) CT-nRT synaptic strength is reduced and cortical information is transmitted directly to the relay thalamus principally via CT-TC pathway (red arrow in a, right panel). (b) In wild-type, direct CT-TC excitation is shunted by CT-nRT-TC feed-forward inhibition. By contrast, in *Gria4*^{-/-}, absence of CT-nRT-TC feed-forward inhibition opens a large window of susceptibility to direct CT-TC excitation, leading to “hyperactivation” of TC cells, which subsequently “hyperexcite” nRT neurons, which in turn inhibit TC neurons, leading to postinhibitory rebound bursts of action potentials in TC-nRT pathway and leading to intrathalamic circuit resonance oscillations (1, green circle). This could lead to hypersynchronous network oscillations within the corticothalamic loop (2, green circle). Red (arrows, synapses and soma) indicate the preferential synaptic pathway of information transfer from cortex to thalamus. The gradient of background color shows balance in synaptic strengths, in favor of CT-nRT pathway in wild-type, but in favor of CT-TC pathway in *Gria4*^{-/-} mice. Thickness of connections is proportional to synaptic or network strength. CT, corticothalamic neuron; Glu, glutamate; nRT reticular thalamic neuron; TC thalamocortical neuron.

Supplementary Table 1. Cutting VB thalamus from slices does not alter electrical membrane properties of nRT neurons in either wild-type or *Gria4*^{-/-} mice.

	Cm (pF)	V _m (mV)	R _{in} (MΩ)	τ _m (ms)	Action pot. threshold (mV)	Action pot. duration (ms)	Action pot. amplitude (mV)	# cells	# slices
WT +VB	64.0 ± 3.0	-68.0 ± 1.7	361.2 ± 24.0	35.2 ± 2.5	-52.3 ± 0.5	1.3 ± 0.1	59.7 ± 1.6	29	17
WT -VB	60.0 ± 4.2	-65.3 ± 2.2	359.01 ± 23.6	36.6 ± 2.4	-52.8 ± 1.3	1.3 ± 0.1	58.3 ± 2.0	13	4
ANOVA	p > 0.1	p > 0.1	p > 0.5	p > 0.5	p > 0.5	p > 0.5	p > 0.5		
<i>Gria4</i> ^{-/-} +VB	55.5 ± 3.4	-67.5 ± 1.8	403.4 ± 37.0	33.5 ± 2.5	-52.2 ± 0.7	1.2 ± 0.1	59.9 ± 1.5	23	13
<i>Gria4</i> ^{-/-} -VB	57.1 ± 4.6	-65.5 ± 2.5	367.3 ± 17.6	30.7 ± 3.7	-52.6 ± 1.0	1.1 ± 0.04	56 ± 2.6	8	5
ANOVA	p > 0.5	p > 0.5	p > 0.5	p > 0.5	p > 0.5	p > 0.1	p > 0.1		

The membrane capacitance (C_m), resting potential (V_m), input resistance (R_{in}), time constant (τ_m) and action potential (pot.) properties of nRT neurons were similar in presence (+) or absence (-) of VB thalamus in both wild-type (n = 8) and *Gria4*^{-/-} (n = 7) mice. All values are expressed as means ± s.e.m.